Journal of Colloid and Interface Science 376 (2012) 289–295

Contents lists available at SciVerse ScienceDirect

Journal of Colloid and Interface Science

www.elsevier.com/locate/jcis

Interaction of chitosan and mucin in a biomembrane model environment

Cristiane A. Silva, Thatyane M. Nobre, Felippe J. Pavinatto, Osvaldo N. Oliveira Jr. *

Instituto de Física de São Carlos, Grupo de Polímeros "Prof. Bernhard Gross", Universidade de São Paulo, 369, São Carlos, SP, Brazil

ARTICLE INFO

Article history:
Received 12 January 2012
Accepted 12 March 2012
Available online 19 March 2012

Keywords:
Cell membrane models
Langmuir monolayers
Chitosan
Mucins
Mucoadhesion

ABSTRACT

Chitosans have been widely exploited in biological applications, including drug delivery and tissue engineering, especially owing to their mucoadhesive properties, but the molecular-level mechanisms for the chitosan action are not known in detail. It is believed that chitosan could affect the mucus by interacting with the proteins mucins, in a process mediated by the cell membrane. In this study we used Langmuir monolayers of dimyristoylphosphatidic acid (DMPA) as simplified membrane models to investigate the interplay between the activity of mucins and chitosan. Surface pressure and surface potential measurements were performed with DMPA monolayers onto which chitosan and/or mucin was adsorbed. We found that the expanding effect from mucin was considerably reduced when chitosan was injected after mucin had been adsorbed on the DMPA monolayer. The results were consistent with the formation of complexes between mucin and chitosan, thus highlighting the importance of electrostatic interactions. Furthermore, chitosan could remove mucin that was co-deposited along with DMPA in Langmuir–Blodgett (LB) films, which could be ascribed to molecular-level interactions between chitosan and mucin inferred from the FTIR spectra of the LB films. In conclusion, the results with Langmuir and LB films suggest that electrostatic interactions are crucial for the mucoadhesive mechanism, which is affected by the complexation between chitosan and mucin.

1. Introduction

There has been a trend toward the use of surface analytical methods to correlate the physiological action of biomolecules and pharmaceutical drugs with their interaction with cell membranes [1–6]. Motivation for such studies arises from the findings that coupling and/or penetration to the membrane are essential for the action of those molecules, especially in cases where the elasticity of the membrane is affected [1,4,5]. For example, infection from protozoa [3] is believed to be triggered by loss of membrane elasticity, and therefore a possible strategy to prevent infection would be to identify drugs that could help restore the membrane elasticity. Obviously, such identification is only possible if molecular-level information is obtained for the biological system under investigation. The study of molecular-level interactions with whole cell membrane is not realistic owing to the difficulties in performing experiments *in vivo*, but one can learn a great deal using model membranes, such as liposomes [7–10], Langmuir monolayers and Langmuir–Blodgett (LB) films [11–20]. In recent years our group has worked extensively with cell membrane models for various types of biologically-relevant molecules [1–5,11–16,18,20], including chitosans.

Chitosan is a natural polysaccharide obtained from deacetylation of chitin. The interest in chitosan stems from its excellent mucoadhesive properties that are explored in many of its biological applications, including vehicles for drug delivery, wound healing devices and tissue engineering [21–28]. The findings with cell membrane models have allowed us to infer that electrostatic interactions may be the most important feature in the chitosan action, but they are not the only relevant ones. Of particular interest are the cases where chitosan action is mediated by other biomolecules. For the mucoadhesive properties of chitosan, for example, it is believed that a major role is played by the protein mucin [29–32], which is the main component of the mucus [33,34] (the biological fluid that covers the surface of body tissues). Mucin is a high molecular weight glycoprotein (10^6–10^7 Da) formed by approximately 75% of oligosaccharides O-linked to protein backbone in the form of *N*-acetylglucosamine, *N*-acetylgalactosamine, fucose, galactose, sialic acid and traces of mannose and sulfate. The primary structure of the protein (approximately 25% of the remaining molecular weight) is composed of serine or threonine residues [35]. Molecular weights from 1.6 to 15 MDa have been reported for porcine stomach and bovine submaxillary gland mucins [36].

The importance of mucin for the mucoadhesive properties of chitosan was inferred from studies involving chitosan–mucin complexation *in vitro* [29–31,37–40]. Even though this complexation takes place very close to the tissue (and hence to the cell membrane) surface, to the best of our knowledge there are no papers

* Corresponding author. Fax: +55 16 3373 9825.
E-mail address: chu@ifsc.usp.br (O.N. Oliveira Jr.).

0021-9797
http://dx.doi.org/10.1016/j.jcis.2012.03.027

in the literature describing how chitosan and mucin interact in a biomembrane environment. In this paper, we use Langmuir films of negatively charged dimyristoylphosphatidic acid (DMPA) as simple cell membrane models, and investigate their interaction with mucin in the presence and absence of chitosan. DMPA was chosen because of its simple structure that may allow one to extrapolate the results to other negative phospholipids, in addition to permitting easy deposition as LB films. The Langmuir films are characterized with surface pressure and surface potential isotherms while the deposition of LB films was monitored with a quartz crystal microbalance.

2. Materials and methods

2.1. Materials

Porcine gastric mucin (PGM), type II (M1778) with bound sialic acids 1% (average M_w 29 MDa), was purchased from Sigma and used as received. Its effective particle diameter (measured by dynamic light scattering) and zeta potential (ζ-Potential) were determined in a Zetatrac (Microtrac) Instrument, using a 780 nm laser. All measurements were performed at 25 °C in triplicate, with the reported values being the average particle diameter ± standard deviation (SD). Chitosan (CS) with a molecular weight of 113,000 Da and a degree of acetylation 19% was obtained from Galena Farmacêutica (Brazil). Prior to use the chitosan was purified by dissolution in diluted HCl (0.1%), followed by filtration and precipitation in a NaOH aqueous solution and washing with ethanol and water until neutrality was achieved. DMPA was purchased from Avanti Polar Lipids. All the other chemicals had analytical grade (>99%). Water used throughout the experiments was supplied by a Milli-Q Integral 10 purification system from Millipore (resistivity 18.2 MΩ cm, pH ~ 6). The Theorell–Stenhagen buffer (TS) solution was prepared with ionic strength of 0.03 mol L^{-1} by dissolving NaOH, citric acid, boric acid and phosphoric acid in water. Its pH was adjusted to 3.0 with the addition of 2 mol L^{-1} HCl, and the surface tension was 73.4 mN m^{-1} at 22 °C.

2.2. Methods

The Langmuir monolayers were prepared on a mini-KSV Langmuir trough (KSV, Finland), total volume of 230 mL housed in a class 10,000 clean room, equipped with a Wilhelmy plate made of a filter paper and a Kelvin probe to measure surface potential. The PGM stock solution at 10 mg mL^{-1} was prepared on the day of the experiment by dissolving the protein in the TS buffer prior to all measurements. Langmuir monolayers of DMPA were obtained by spreading a chloroform solution of DMPA (0.5 mg mL^{-1}) on the TS buffer subphase. Mixed monolayers of PGM and DMPA were prepared by injecting a PGM aqueous solution in the subphase to obtain a final concentration of 0.1 mg mL^{-1} just below the interface, after the DMPA spreading. After the adsorption equilibrium was attained the monolayers were compressed. The effect from chitosan was evaluated using two methodologies. In the first, a mixture of PGM and CS solutions was dissolved in 230 mL of TS buffer to obtain a final concentration of 0.1 mg mL^{-1} PGM and 0.1 mg mL^{-1} CS at 1:1 w/v proportion and employed as a subphase for spreading the DMPA monolayer (Methodology 1). In the second methodology, after complete adsorption of PGM onto a DMPA interface, aliquots of chitosan stock solution (5 mg mL^{-1}) were injected into the subphase to obtain a final concentration of 0.1 mg mL^{-1} CS (Methodology 2). Surface pressure–area (π–A) and surface potential–area (ΔV–A) isotherms were obtained with a monolayer compression rate of 10 mm min^{-1} (trough surface area of 75 × 323 mm^2), with the subphase at 21 ± 1 °C.

The transfer of DMPA, PGM/DMPA and PGM:CS/DMPA monolayers onto solid supports was performed at a constant surface pressure of 35 mN m^{-1}, at 22 °C with a dipping speed from 0.2 to 2 mm min^{-1}, which rendered a transfer ratio closed to 1.2 in Y-type LB films. The supports used were silicon for infrared spectroscopy and AT-cut quartz crystal coated with Au on a 0.4 cm^2 active area (Stanford Research Systems, Inc.) with a fundamental frequency of ca. 5 MHz for QCM nanogravimetry. The first layer was deposited during the upstroke, and 30 min elapsed to allow the film to dry before transferring the second layer in the downstroke. The presence of DMPA, PGM and CS in the LB films was inferred from transmission Fourier transform infrared spectroscopy (FTIR) measurements with a Thermo Nicolet Nexus 470 spectrometer and QCM (Stanford Research Systems, Inc.). The oscillation frequencies in the QCM measurements were monitored until equilibrium was reached. Changes in the oscillation frequencies are taken as proportional to the adsorbed mass, according to the Sauerbrey equation [41], $\Delta f = -c_f \Delta m$, where Δf is the observed frequency change in Hz, c_f is the sensitivity factor for the crystal (56.6 Hz μg^{-1} cm^{-2} for a 5 MHz crystal at room temperature) and Δm is the change in mass per unit area, in g cm^{-2}. All experiments were carried out in triplicate.

3. Results and discussion

There are several parameters to investigate in analyzing the interaction between biomolecules and cell membrane models. With mucins being proteins from the gastric system, low pHs are suitable to reproduce the environment surrounding the proteins, which is convenient because chitosans are soluble at such pHs. PGM is uncharged at pH 2, but acquires negative charge at pH > 2 [42]. PGM forms stable suspensions at low concentrations (1 mg/mL), which could be characterized using dynamic light scattering and ζ-Potential measurements. Table 1 points to a bimodal distribution of PGM particles. Furthermore, chitosan causes aggregation thus leading to PGM:CS complexes in large aggregates, consistent with the literature [30]. From the ζ-Potential, also shown in Table 1, we infer that PGM particles had net negative surface charge at pH 3 (−3 mV), while the PGM:CS complex particles had a positive potential of 28 mV, thus confirming the adsorption of cationic molecules on the surface. This was expected because at pH 3 the amino groups of chitosan are protonated.

Since the main purpose here is to verify whether chitosan affects the interaction between mucin (PGM) and Langmuir monolayers of DMPA, the first step was to check whether PGM adsorbs on different interfaces. Fig. 1a shows the adsorption kinetics for PGM dissolved into a buffer solution (pH 3.0) without chitosan onto a clean air/buffer interface. After an induction time of ca. 200 min, which can be ascribed to a diffusive process, the surface pressure increased up to ca. 6 mN m^{-1} approximately 14 h after the PGM injection, after which no significant change in surface pressure was observed. When PGM was injected under a preformed DMPA monolayer, the induction time was shorter, ca. 120 min (Fig. 1b). In both cases, after 14 h of experiment the surface pressure tended to level off. However, the most important evidence is the decrease or disappearance of the lag time for adsorption when PGM forms a complex with chitosan (PGM:CS)

Table 1
Dynamic light scattering and ζ-Potential measurements for pig gastric mucin (1 mg/mL) and pig gastric mucin:chitosan complex (1:1 w/v) at pH 3.

	Effective particle diameter ± SD (nm)	ζ-Potential (mV)
PGM	1306 ± 140 and 262 ± 78	−3 ± 2
PGM:CS complex	2795 ± 247 and 478 ± 112	28 ± 2

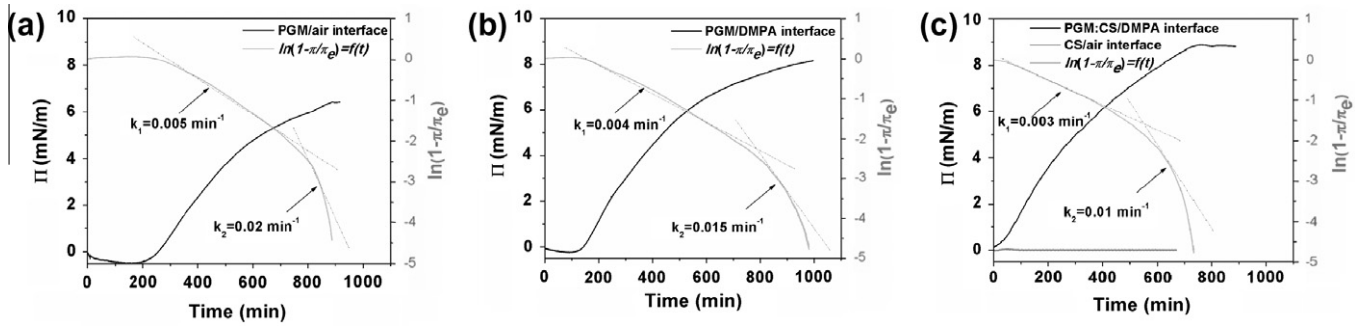

Fig. 1. Kinetics of adsorption for PGM (0.1 mg mL^{-1}) at the air/Theorell–Stenhagen interface (Na^+ 0.03 mol L^{-1} pH 3) (a), at a DMPA monolayer (b) and for chitosan (0.1 mg mL^{-1}) at a PGM/DMPA monolayer (c). Note that chitosan on its own does not adsorb on a bare interface.

(Methodology 1), as shown in Fig. 1c. The increase in surface pressure due to adsorption of PGM:CS complex into a preformed DMPA monolayer was approximately 2 mN m^{-1} higher than the corresponding value for a neat air/TS buffer interface. Similar results with other proteins have indicated that protein adsorption is enhanced when phospholipid molecules are at the air/liquid interface [43,44]. The differences observed here are nevertheless small, as will be commented upon later on.

The kinetics data in Fig. 1 were treated quantitatively with the approach by Magett-Dana [43] who applied a first-order equation [45], $ln(\Pi_e - \Pi/\Pi_e - \Pi_0) = -kt$, to analyze adsorption of proteins on liquid interfaces, where Π_e, Π and Π_0 are the surface pressure values at steady-state condition, at a time t and at time $t = 0$, respectively, and k is the rate constant. The plots for $ln(1 - \Pi/\Pi_e) = f(t)$ in Fig. 1 share a common feature in that they can be divided into three parts: an induction period and two other parts that may be approximated by straight lines. Using regression analysis, two rate constants were identified, namely k_1 for the first part and k_2 for the latter part. According to Magett-Dana [43], the rate constant k_1 is related to the protein incorporation and possibly unfolding onto the surface layer while k_2 is associated with the rearrangement of the adsorbed protein molecules. k_1 was 0.004 min^{-1} for the three types of interface, while k_2 was 0.017, 0.014 and 0.011 min^{-1}, for PGM/air, PGM/DMPA and PGM:CS/DMPA interfaces, respectively. Therefore, k_1 is not sensitive to the kind of interface, but k_2 decreased considerably with DMPA at the interface because PGM molecules had to rearrange themselves among the DMPA molecules. Furthermore, since PGM could not be inserted into a DMPA monolayer in the first two hours of experiment (Fig. 1b), but could do in the first minutes when forming a complex with chitosan (Fig. 1c), one believes there is strong interaction between PGM and chitosan with DMPA monolayers.

The effective adsorption of PGM onto a DMPA monolayer does affect the surface pressure and surface potential isotherms of the lipid, as illustrated in Fig. 2a and b. In these experiments, the isotherms were measured ca. 14 h after injecting PGM a few millimeters below the surface onto which a DMPA monolayer had been spread. The isotherms for pure DMPA spread on the TS buffer are more expanded than on pure water [46], as DMPA is sensitive to the ions in the subphase [47]. PGM causes a large expansion in the isotherms, which points to penetration of PGM molecules into the monolayer for large areas per molecule, resulting in a monolayer with a high compressibility or low compressional modulus, C_s^{-1}, defined as $-A(d\pi/dA)$, where A is the molecular area [48]. For instance, at the surface pressure of 30 mN m^{-1}, C_s^{-1} is 160 mN m^{-1} for pure DMPA and ca. 20 mN m^{-1} for the four PGM concentrations used. The smaller elasticity of the PGM/DMPA film at a high surface pressure may be attributed to the insertion of PGM molecules into the hydrophobic tail regions of the DMPA monolayer at considerable pressures that would be equivalent to a real membrane (believed to be ca. 30 mN m^{-1}) [49]. In all cases, the collapse pressure is the same as for a DMPA neat monolayer. Before the curves coincide at the collapse, even at high surface pressures the areas per DMPA molecule are much larger in the presence of PGM. Because DMPA has a negatively charge polar head, electrostatic interactions with the positive residues of PGM could be a major component for the effects. However, the slightly negative ζ-Potential for PGM indicates that hydrophobic and secondary interactions should predominate. Accordingly, the adsorption of PGM onto a DMPA monolayer at low surface pressure should occur in a way that the non-glycosylated domains of mucins act as binding sites through their hydrophobic interactions with the DMPA interface, while hydrophilic carbohydrates may dangle out to interact with the subphase. With regard to

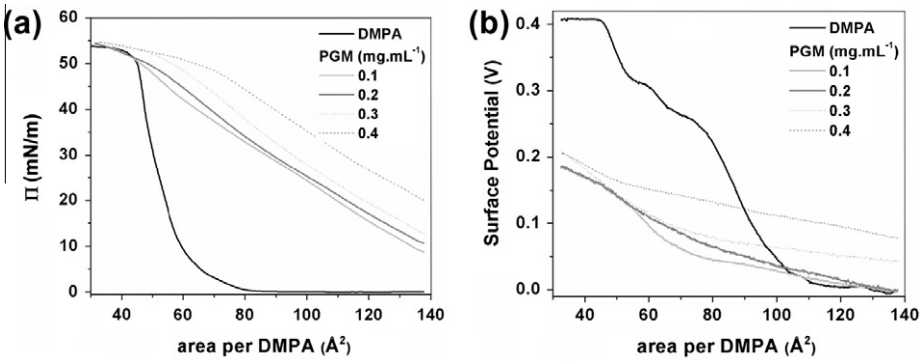

Fig. 2. (a) Surface pressure–area (Π–A) and (b) surface potential–area (ΔV–A) isotherms for DMPA with several PGM concentrations in the subphase.

measurements with zwitterionic phospholipids, dipalmitoylphosphatidylcholine (DPPC), in subsidiary experiments (*data not shown*) we observed that mucin was expelled from the interface when the DPPC monolayer was compressed to high surface pressures.

The adsorption of PGM on the DMPA monolayer caused the surface potential to decrease for small areas per molecule, as indicated in Fig. 2b, whereas the potential increased slightly at large areas per molecule. In a complex system containing DMPA molecules and adsorbed PGM it is impossible to predict the surface potential quantitatively, as the charge distribution and dipole orientation are unknown. Nevertheless, the considerably lower surface potential at small areas per molecule indicate that the incorporation of PGM molecules causes the positive contributions from the dipole moments of DMPA molecules to decrease substantially, probably because the packing is affected. Another possibility would be a decrease in surface potential owing to a change in surface charge of the DMPA monolayer, induced by PGM. However, this explanation is not consistent with the higher surface potential for PGM-containing monolayers at large areas per molecule, where the contribution from the electrical double-layer should dominate. Moreover, PGM was shown to be only slightly negative and would not be able to alter the DMPA surface charge to any significant extent. One may conclude, therefore, that a change in the packing of DMPA molecules should indeed be the most likely explanation for the decrease in potential. This hypothesis is consistent with the very distinct elasticity of the DMPA monolayer onto which PGM was adsorbed, in comparison to a neat DMPA monolayer.

The expansion in the surface pressure isotherms with increasing PGM concentration is best illustrated in the plots of area per DMPA molecule at a fixed surface pressure of 30 mN/m or by the change in pressure at a fixed area of 80 Å^2, both depicted in Fig. 3. After a sharp increase at low PGM concentrations, the effects tended to level off for higher concentrations, as saturation takes place.

To evaluate the effects from chitosan (CS) on PGM/DMPA films, two methodologies were used. In the first one, the subphase for spreading the DMPA monolayer contained both PGM and CS in a 1:1 w/v proportion (Methodology 1). The surface pressure isotherms were taken after approximately 14 h of experiment where no significant variation was observed in surface pressure. As shown in Fig. 4a, the surface pressure isotherm almost coincided with that with only PGM in the subphase. For the surface potential isotherms, Fig. 4b shows some increase in potential for the PGM:CS mixture. Major effects, however, appeared in the second methodology, in which CS 0.1 mg mL^{-1} was injected into the subphase 14 h after injecting PGM 0.1 mg mL^{-1} under a preformed DMPA monolayer (Methodology 2). In the surface pressure isotherms in Fig. 4a, there is apparently some removal of material in the liquid-condensed phase. Furthermore, the incorporation of CS had a "recharging" effect on PGM, causing the significant increase in surface potential in Fig. 4b. These results are consistent with the dynamic light scattering data reported by Sogias et al. [30] where aggregation of PGM was observed in the presence of chitosan and its half-acetylated derivative. They also reported that the chitosans recharged the mucin particles, confirmed with adsorption of cationic macromolecules on their surfaces. The increase in aggregation and a positive surface charge were both confirmed by our DLS and zeta potential results, reported in Table 1. We therefore believe that PGM and CS form a complex since protonated CS has positively charged primary amino groups in the pH used (3.0) that may interact electrostatically with the negatively charged PGM macromolecules. Indeed, rather than displaying a surface potential smaller than for neat DMPA, with CS injected (Methodology 2) into the PGM-containing subphase the potential was even higher. Further analysis of the surface potential data will be done when a model for the interaction is introduced later on in this Section. Note also that the chitosan concentration (0.1 mg mL^{-1}) used in this study is diluted with no steep increase in bulk viscosity. No surface activity was detected, as the surface tension was not altered when the barriers (without protein) were compressed with chitosan in the subphase, which may be explained by the high solubility of chitosan at a low pH.

Attempts were made to produce Langmuir–Blodgett (LB) films from the systems studied here. We found that PGM could be transferred together with DMPA onto a solid substrate, as indicated by the QCM data in Table 2. However, when chitosan was in the subphase, either mixed with PGM from the start (Methodology 1) or injected into a PGM-containing subphase (Methodology 2), transfer occurred only in special cases. In fact, for CS injected in the second experiment no PGM could be transferred to either the silicon or the QCM gold substrate, which may be evidence for the formation of PGM:CS complexes. For CS mixed with PGM (Methodology 1), deposition was possible on silicon but not on gold. It seems that chitosan sequestrates PGM, which hampers deposition. This hypothesis was confirmed in further experiments in which LB films made with four layers of PGM/DMPA were immersed into a buffer solution containing CS, to be discussed below.

The transfer of PGM onto LB films was confirmed with measurements with a quartz crystal microbalance (QCM). Three layers of neat DMPA and one layer of PGM/DMPA were adsorbed on the gold-coated QCM quartz crystal with deposition at a surface pressure of 35 mN m^{-1}. The transfer ratio was approximately 1.2 for all cases, which confirm the quality of deposition. The results are shown in Table 2 and Fig. 5 with the deposited mass calculated with the Sauerbrey equation [41]. The mass deposited of a single layer of neat DMPA is 178 ng, while for the PGM/DMPA layer the mass was 968 ng. The mass increase in relation to the value for a DMPA film should correspond to PGM effectively interacting with DMPA. A fifth layer made of chitosan was deposited by immersion of the PGM/DMPA LB film in 1 mg mL^{-1} solution of chitosan. In previous studies with DMPA monolayers spread onto chitosan-containing subphases, it has been shown that even in cases where chitosan is believed to be expelled from the interface, no longer contributing to the area per lipid molecule in a condensed monolayer, it is still possible to transfer chitosan together with DMPA in an LB film [15,14,18]. This is so because chitosan is located on a subsurface of the monolayer. When the LB film was rinsed with the buffer solution, after chitosan adsorption, the mass decreased by 466 ng. However, if the buffer solution also contained chitosan, then the decrease in mass was much more significant, yielding zero mass after 120 min. This indicates that chitosan sequestrates PGM from the LB film to such an extent that even the DMPA molecules were desorbed, thus destroying the film.

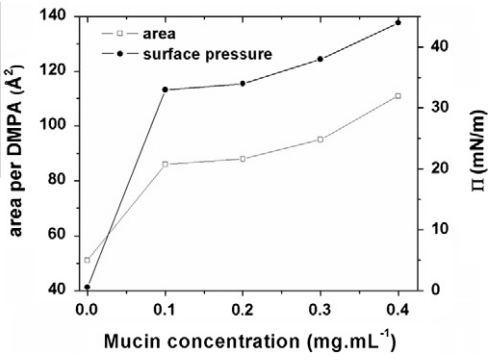

Fig. 3. Area per phospholipid molecule at 30 mN m^{-1} (●) and surface pressure at 80 Å^2 (□) versus mucin concentration in the subphase for DMPA monolayer.

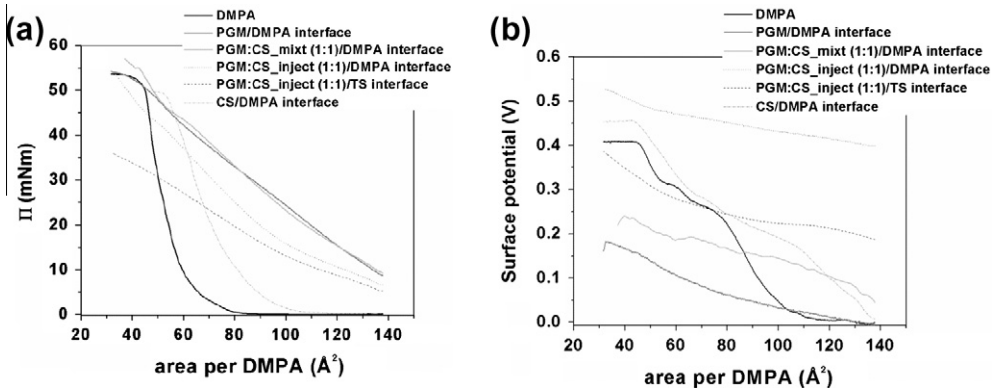

Fig. 4. (a) Surface pressure–area (Π–A) and (b) surface potential–area (ΔV–A) isotherms for DMPA with mucin and mucin-chitosan mixture in the subphase.

Table 2
QCM results for DMPA LB films. In the first immersion of the PGM/DMPA LB film into the chitosan solution some adsorption occurred, causing the mass to increase. However, in subsequent immersions the mass decreased owing to the desorption of PGM and even of DMPA induced by chitosan.

Layer type	Mass per layer (ng)
DMPA	178
DMPA/PGM	968
1st immersion of PGM/DMPA LB film in chitosan solution	1200
2th immersion	734
3rd immersion	297
4th immersion	198
5th immersion	89
6th immersion	71
7th immersion	21
8th immersion	21

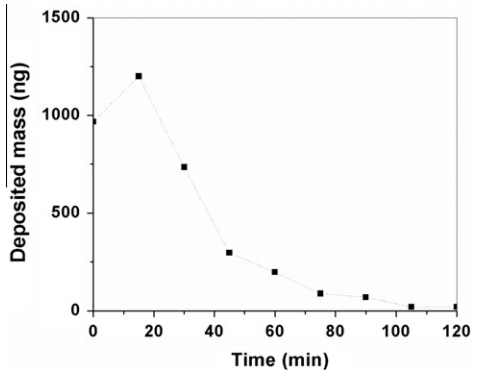

Fig. 5. Kinetics of desorption and adsorption of chitosan on a PGM/DMPA LB film. The measurements were carried out by successive immersions of PGM/DMPA LB film in a chitosan solution during adequate time intervals, with subsequent withdrawal and drying.

The PGM/DMPA and PGM:CS_{mixt}/DMPA (Methodology 1) LB films deposited on silicon substrates displayed FTIR spectra featuring the bands typical of CS and PGM, in addition to those of DMPA. This is illustrated in Fig. 6, where a comparison is made between these LB films and cast films of DMPA, CS and PGM. The main bands for a cast DMPA film in the region between 3500 and 2800 cm^{-1} in Fig. 6a were assigned to the asymmetric stretching of CH_3 at 2940 cm^{-1}, and asymmetric and symmetric stretching modes of CH_2, at 2903 and 2835 cm^{-1}, respectively. This spectrum is consistent with the literature [50]. In the spectrum for the PGM cast film, the main bands were assigned to N—H and O—H stretching modes at 3304 cm^{-1} and 2914, respectively and 2843 cm^{-1} assigned to C—H stretching modes, also consistent with the literature [51]. The spectrum of chitosan shows an amide II and a C=O stretching band at 1557 and 1711 cm^{-1}, respectively (Fig. 6b). For the PGM/DMPA LB film, a band appears at 3290 cm^{-1} assigned to the stretching of N—H and O—H groups from PGM (Fig. 6a). These results confirm that PGM must be at the interface. The shift in CH_2 vibrational bands of DMPA in the presence of PGM is probably due to the increased number of conformers along the lipid chains. Another possible cause for the shift is nonhomogeneous phases. The phase transition during monolayer compression may lead to microdomains, thus affecting orientation of DMPA chains at air/TS interface. For the PGM:CS/DMPA LB film, the band at 3253 cm^{-1} assigned to N—H and O—H groups is shifted in comparison to the spectra of PGM and CS. This should be ascribed to intermolecular interactions between PGM and CS. The spectrum of PGM showed a C=O stretching band of an amide band at 1726 cm^{-1}. The C=O absorption band was shifted to 1709 cm^{-1} in the PGM:CS/DMPA spectrum, again indicating interactions between CS and PGM in the LB film.

3.1. Possible models for PGM interactions

Most proteins have an amphiphilic character due to their hydrophobic aminoacid residues, and may therefore be surface active. The presence of a lipid monolayer can improve adsorption at the interface, since the monolayer can provide a more hydrophobic environment. In some cases, adsorption is guided by specific interactions (between some chemical groups) in the lipid that the protein is able to recognize. Taken all the results presented here together, PGM probably interacts with the DMPA monolayer via hydrophobic interactions, which explains why PGM adsorption was not much stronger than on a bare interface (with no DMPA). The addition of chitosan to the subphase promotes electrostatic interaction between PGM and chitosan, and this strong interaction is able to remove the protein from the interface. A model for this phenomenon is shown in Fig. 7. This action of chitosan is specific for model membranes made with negatively charged phospholipids, and is similar to what was reported for β-lactoglobulin (BLG) [15], where BLG could be incorporated into negatively charged phospholipid monolayers at the air–water surface, but it was removed when chitosan was injected after the saturation of BLG adsorption. This removal occurred for the negatively charged DMPA, but not for cholesterol and zwitterionic phospholipids. Therefore, electrostatic interactions are crucial for the removal mechanism. We should stress that in the results for Langmuir

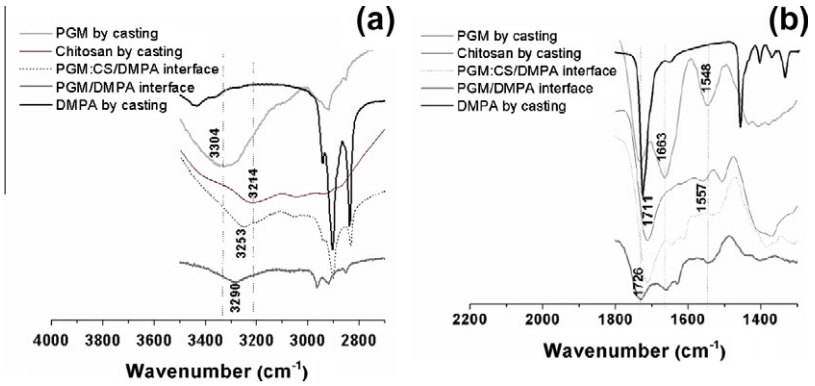

Fig. 6. FTIR spectra for DMPA, PGM and PGM/DMPA films. (a) from 3500 to 2700 cm^{-1} and (b) from 1800 to 1500 cm^{-1}.

monolayers the model in Fig. 7 applies only to the experiments performed in Methodology 2, with injection of chitosan after adsorption of PGM at the interface.

A comparison of the results for the two methodologies points to a competition of effects. For PGM can either bind to the monolayer (membrane) or form a complex with chitosan. With the data in Methodology 2, it is clear that complexation is preferred since the PGM molecules adsorbed on the DMPA interface were removed upon injection of chitosan in the subphase. As for the results in Methodology 1, the chitosan-PGM complex has positive ζ-Potential and therefore may interact with the DMPA monolayer via electrostatic and hydrophobic interactions, thus increasing the probability of adsorption which may explain the absence of lag time. The competing interactions among DMPA, chitosan and PGM have led to completely different molecular organizations in the two methodologies, which were reflected on very distinct surface potential isotherms in Fig. 4b, as the surface potential depends strongly on the molecular organization at the air/water interface.

4. Conclusions

Mucin has a strong affinity for a simple biomembrane composed of negatively charged phospholipid, as proven here using Langmuir monolayers of DMPA as models. Mucin could be inserted into the monolayer thus causing a large expansion in the isotherms, which was accompanied by a decrease in surface elasticity. Mucin probably interacts with the DMPA monolayer via hydrophobic interactions. Chitosan is not surface active, but it formed a complex with mucin, and this complex adsorbed on the DMPA monolayer much in the same way as pure mucin. In contrast, when chitosan was added to the subphase after the saturation of mucin adsorption, the extent of monolayer expansion was reduced. The addition of chitosan promotes electrostatic interaction between mucin and chitosan, and this strong interaction is able to remove the protein from the interface. This finding was confirmed in LB films experiments, where chitosan was able to gradually remove the protein, in addition to DMPA molecules.

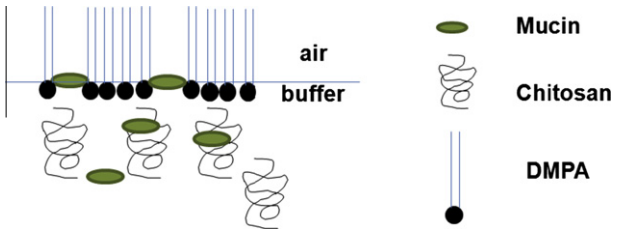

Fig. 7. Model for the pig gastric mucin removal from negatively charged phospholipid monolayers caused by chitosan.

Perhaps the most important biological implication of this study is associated with the hypothesis that chitosan may affect mucoadhesion. Indeed, mucin had a dramatic influence on chitosan action over biomembranes. If the results presented here were to be valid in real membranes, for human tissues covered by mucus, chitosan would primarily form complexes with the protein and the resulting colloids cause greater impact on cell membrane elasticity and surface charge. The electrostatic interactions with negatively charged phospholipids on the cell surface are believed to govern chitosan action, as indicated in studies with liposomes and Langmuir monolayers as cell membrane models [10,18,52]. However, the tendency of chitosan to form complexes with mucin and other proteins seems to surpass its ability of binding to membranes, with the resulting complexes causing major disturbances in the membrane. Understanding the mechanisms for the action of chitosan may also be crucial in biological applications, as the mucus can act as a barrier for chitosan when it migrates to the surface of living tissues.

Acknowledgments

This work was supported by FAPESP, CNPq, CAPES and rede nBioNet (Brazil).

References

[1] T.M. Nobre, F.J. Pavinatto, M.R. Cominetti, H.S.S. Araújo, M.E.D. Zaniquelli, L.M. Beltramini, Biochim. Biophys. Acta 1798 (2010) 1547.
[2] T.E. Goto, R.F. Lopez, O.N. Oliveira Jr., L. Caseli, Langmuir 26 (2010) 11135.
[3] C.P. Pascholati, E.P. Lopera, F.J. Pavinatto, L. Caseli, T.M. Nobre, M.E.D. Zaniquelli, T. Viitala, C. D'Silva, O.N. Oliveira Jr., Colloid. Surf. B 79 (2009) 504.
[4] L. Caseli, A.C. Perinotto, T. Viitala, V. Zucolotto, O.N. Oliveira Jr., Langmuir 25 (2009) 3057.
[5] F.J. Pavinatto, A. Pavinatto, L. Caseli, D.S. dos Santos, T.M. Nobre, M.E.D. Zaniquelli, T. Viitala, O.N. Oliveira Jr., Biomacromolecules 8 (2007) 1633.
[6] T.J. Millar, S.T. Tragoulias, P.J. Anderton, M.S. Ball, F. Miano, G.R. Dennis, P. Mudgi, Cornea 25 (2006) 91.
[7] C. Peetla, A. Stine, V. Labhasetwar, Mol. Pharm. 6 (2009) 1264.
[8] N.J. Wittenberg, L. Zheng, N. Winograd, A.G. Ewing, Langmuir 24 (2008) 2637.
[9] F. Quemeneur, M. Rinaudo, B. Pepin-Donat, Biomacromolecules 9 (2008) 2237.
[10] N. Fang, V. Chan, Biomacromolecules 4 (2003) 581.
[11] F.J. Pavinatto, L. Caseli, O.N. Oliveira Jr., Biomacromolecules 11 (2010) 1897.
[12] E.A. Montanha, F.J. Pavinatto, L. Caseli, O. Kaczmarek, J. Liebscher, D. Huster, O.N. Oliveira Jr., Colloid. Surf. B 77 (2010) 161.
[13] T.F. Schmidt, F.J. Pavinatto, L. Caseli, M.L.C. Gonzaga, S.A. Soares, N.M.P.S. Ricardo, O.N. Oliveira Jr., J. Colloid Interface Sci. 339 (2009) 84.
[14] F.J. Pavinatto, C.P. Pacholatti, E.A. Montanha, L. Caseli, H.S. Silva, P.B. Miranda, T. Viitala, O.N. Oliveira Jr., Langmuir 25 (2009) 10051.
[15] L. Caseli, F.J. Pavinatto, T.M. Nobre, M.E.D. Zaniquelli, T. Viitala, O.N. Oliveira Jr., Langmuir 24 (2008) 4150.
[16] L. Caseli, F.N. Crespilho, T.M. Nobre, M.E.D. Zaniquelli, V. Zucolotto, O.N. Oliveira Jr., J. Colloid Interface Sci. 319 (2008) 100.
[17] P. Wydro, B. Krajewska, K. Hac-Wydro, Biomacromolecules 8 (2007) 2611.

[18] F.J. Pavinatto, L. Caseli, A. Pavinatto, D.S. dos Santos, T.M. Nobre, M.E.D. Zaniquelli, H.S. Silva, P.B. Miranda, O.N. Oliveira Jr., Langmuir 23 (2007) 7671.
[19] H. Parra-Barraza, M.G. Burboa, M. Sanchez-Vasquez, J. Juarez, F.M. Goycoolea, M.A. Valdez, Biomacromolecules 6 (2005) 2416.
[20] M.L. Moraes, C. Bonardi, C.R. Mendonça, P.T. Campana, J.T. Lottersberger, G. Tonareli, O.N. Oliveira Jr., L.M. Beltramini, Colloid. Surf. B 41 (2005) 15.
[21] R.AA. Muzzarelli, Carbohydr. Polym. 76 (2009) 167.
[22] I.-Y. Kim, S.-J. Seo, H.-S. Moon, M.-K. Yoo, I.-Y. Park, B.-C. Kim, C.-S. Cho, Biotechnol. Ad. 26 (2008) 1.
[23] G.Y. Park, S. Mun, Y. Park, S. Rhee, E.A. Decker, J. Weiss, D.J. McClements, Y. Park, Food Chem. 104 (2007) 761.
[24] M.N.V.R. Kumar, R.A.A. Muzzarelli, C. Muzzarelli, H. Sashiwa, A.J. Domb, Chem. Rev. 104 (2004) 6017.
[25] E.I. Rabea, M.E.-T. Badawy, C.V. Stevens, G. Smagghe, W. Steurbaut, Biomacromolecules 4 (2003) 1457.
[26] S.G. Kumar, M.A. Rahman, S.H. Lee, H.S. Hwang, H.A. Kim, J.W. Yun, Proteomics 9 (2009) 2149.
[27] M. Sumiyoshi, Y.J. Kimura, Pharm. Pharmacol. 58 (2006) 201.
[28] A.K. Singla, M.J. Chawla, Pharm. Pharmacol. 53 (2001) 1047.
[29] N.A. Peppas, Y. Huang, Adv. Drug Deliver. Rev. 56 (2004) 1675.
[30] I.A. Sogias, A.C. Williams, V.V. Khutoryanskiy, Biomacromolecules 9 (2008) 1837.
[31] A. Dedinaite, M. Lundin, L. Macakova, T. Auletta, Langmuir 21 (2005) 9502.
[32] O. Svensson, L. Lindh, M. Cardenas, T. Arnebrant, J. Colloid Interface Sci. 299 (2006) 608.
[33] X. Cao, R. Bansil, K.R. Bhaskar, B.S. Turner, J.T. LaMont, N. Niu, N.H. Afdhal, Biophys. J. 76 (1999) 1250.
[34] A. Allen, Physiology of the Gastrointestinal Tract, Raven Press, New York, 1981.
[35] R. Bansil, E. Stanley, J.T. LaMont, Annu. Rev. Physiol. 57 (1995) 635.
[36] T. Sandberg, H. Blom, K.D. Caldwell, J. Biomed. Mater. Res. A 91A (2009) 762.
[37] I.P. Kaur, R. Smitha, Drug Dev. Ind. Pharm. 28 (2002) 353.
[38] S. Rossi, F. Ferrari, M.C. Bonferoni, C. Caramella, Eur. J. Pharmaceut. Sci. 10 (2000) 251.
[39] M.P. Deacon, S.S. Davis, R.J. White, H. Nordman, I. Carlstedt, N. Errington, A.J. Rowe, S.E. Hardin, Carbohyd. Polym. 38 (1999) 23.
[40] I. Fiebrig, S.E. Harding, A.J. Rowe, S.C. Hyman, S.S. Davis, Carbohyd. Polym. 28 (1995) 239.
[41] G.Z. Sauerbrey, Z. Phys. 155 (1959) 206.
[42] S. Lee, M. Muller, K. Rezwan, N.D. Spencer, Langmuir 21 (2005) 8344.
[43] R. Maget-Dana, Biochim. Biophys. Acta 1462 (1999) 109.
[44] V. Rosilio, M.-M. Boissonnade, J. Zhang, L. Jiang, A. Baszkin, Langmuir 13 (1997) 4669.
[45] D.G. Graham, M.C. Phillips, J. Colloid Interface Sci. 70 (1979) 403.
[46] R.C. Ahuja, P.L. Caruso, D. Mobius, Langmuir 9 (1993) 1534.
[47] M. Losche, C. Helm, H.D. Mattes, H. Mohwald, Thin Solid. Films 133 (1985) 51.
[48] J.T. Davies, E.K. Rideal, Interfacial Phenomena, Academic Press, New York, 1963.
[49] D. Marsh, Biochim. Biophys. Acta 1286 (1996) 183.
[50] A.J. Fernandez, J.J. Ruiz, L. Camacho, M.T. Martin, E.J. Munoz, Phys. Chem. B 104 (2000) 5573.
[51] L. Chiriboga, P. Xie, V. Vigorita, D. Zarou, D. Zakim, M. Diem, Biospectroscopy 4 (1998) 55.
[52] V.G. Babak, G.A. Vikhoreva, I.G. Lukina, Colloids Surf., A 128 (1997) 75.